

## Scaling of diffusion-mediated island growth in iron-on-iron homoepitaxy

Joseph A. Stroschio and D. T. Pierce

*Electron Physics Group, National Institute of Standards and Technology, Gaithersburg, Maryland 20899*

(Received 6 December 1993)

An analysis of the island size and separation distributions of Fe islands, observed in the initial stages of growth in the homoepitaxy of Fe on Fe(001) whiskers, shows scaling properties recently predicted in nucleation and growth theories. A critical size of one atom, where islands greater than the critical size undergo irreversible nucleation, is supported by the measured scaling functions for the Fe on Fe system in the temperature range of 20–250 °C.

Understanding the processes of nucleation and growth is central to growing high-quality materials by molecular-beam epitaxy. On a microscopic scale, we would like to know how atoms diffuse on a surface, after being deposited at random from an impinging flux, and how then they are incorporated in the growing material.<sup>1</sup> Random deposition of atoms drives a system into non-equilibrium, with an initial higher than equilibrium concentration of adatoms. An adatom, or monomer, then undergoes a random walk and has two alternatives that determine its fate; (1) the monomer may find an existing island and become incorporated leading to growth, or (2) it may find one or more other diffusing atoms and nucleate a new island. This new island may be stable or unstable against dissociation depending on the binding energy of the cluster and the surface temperature. In traditional growth theories,<sup>2</sup> the size  $i$  at which an island consisting of  $i$  or less atoms is unstable, but  $i + 1$  atoms is stable, is labeled the critical size. In general the critical nucleus size  $i$  will depend on temperature.

Historically, information on island nucleation has been obtained by scanning electron microscopy and analyzed by nucleation theories based on rate equation treatments of growth.<sup>2,3</sup> More recently, microscopic measurements by scanning tunneling microscopy (STM) have demonstrated the ability to extract diffusion parameters and activation energies from an analysis of the initial stages of island nucleation.<sup>4–6</sup> These recent STM measurements at near room temperature have revealed the evolution of far-from-equilibrium structures.<sup>4–7</sup> In this far-from-equilibrium regime, the rate of escape of an atom from an island is negligible compared to the surface diffusion rate; thus the nucleation of islands is virtually irreversible. This ability to look at the earliest stages of nucleation and growth has started a revival of interest in this field. To formulate a more general description of nucleation and growth and stimulated by these measurements, recent theories have emphasized the scaling of various functions of the initial island distributions, including the density, size, and separation distribution for the case of irreversible island nucleation.<sup>8–12</sup>

In this paper we present results which verify the recent far-from-equilibrium scaling predictions of Bartelt and Evans<sup>9</sup> for the island size and separation distributions as a function of the ratio of the diffusion to deposition rate. The resulting scaling functions for the growth of Fe on Fe(100) closely resemble the predictions for a critical nu-

cleus size  $i = 1$ .<sup>10</sup> Measurements of the island density and size distributions at temperatures above 250 °C show a change from the initial scaling function to a second scaling relation, which can be interpreted as an increase in the critical size for nucleation in this temperature range.

The experiments were performed in an ultrahigh vacuum system with STM and reflection high-energy electron diffraction (RHEED) measurement capability and facilities for metal film growth, described elsewhere.<sup>13</sup> Fe was evaporated using an Fe wire wound on a tungsten filament with the substrate held at a selected temperature. The sample was then cooled after growth was stopped at a rate of about one degree per second. Subsequent analysis was made by STM measurements at room temperature, where the frozen-in configurations, at the point where growth was interrupted, were observed. Single-crystal Fe whiskers, cleaned by sputtering at 750 °C, were used for substrates. STM measurements on the whisker surfaces showed extremely flat surfaces with typical terraces 1  $\mu\text{m}$  or larger in length, which allow the analysis of nucleation events without any complications due to step structures.

Figure 1 shows a selection of STM images of the initial stages of growth of single-atom-high Fe islands as a function of substrate temperature. The Fe deposition was held at a fixed rate (flux per lattice site)  $r$  for a fixed time, to yield the same integrated flux (or coverage  $\Theta$ ) in each image. A number of features are apparent from the images in Fig. 1. First the propensity towards island growth versus nucleation increases with increasing temperature. Growth and nucleation are competing processes, and since the adatom diffusion increases with temperature, the probability for an atom to find an existing island instead of nucleating a new one increases. The second feature to notice is the self-similarity of the island distributions with change in temperature; this can be seen qualitatively by comparing Figs. 1(a)–1(c) with 1(d)–1(f) and noting the change in scale. The third feature to notice is that there is a characteristic region around each island which is void of other islands. We now analyze these features more closely.

In Fig. 1 we observe a marked decrease in island density with increasing temperature due to an increase in the adatom diffusion. A measure of the diffusion constant and activation energy for diffusion can be obtained from the analysis of the temperature dependence of the island density, if the critical nucleus size is known.<sup>2,10</sup> In the

low-coverage limit for isotropic diffusion, the total density of islands  $N$  varies as<sup>2,10</sup>

$$N \sim \eta(\Theta)(r/\nu)^{\chi} \exp[\chi(E_d + E_i/i)/k_B T], \quad (1)$$

where  $\eta(\Theta) \sim \Theta^{1/(i+2)}$ , and  $\chi = i/(i+2)$ . The diffusion constant is given by  $D = D_0 \exp(-E_d/k_B T)$ , where  $E_d$  is the activation energy for diffusion.  $E_i$  is the binding energy for critical islands of size  $i$ . The diffusion rate is related to the number of jumps an atom makes per second, the hopping rate  $h$  by  $D = ha^2$ , where  $a$  is the lattice constant, and  $D_0 = \nu a^2$ , where  $\nu$  is the attempt frequency. An analysis of the island density for temperatures below 250°C, shown in the inset in Fig. 3(b) below, was recently reported<sup>5</sup> with the assumption of a critical size of 1; an activation energy of  $E_d = 0.45 \pm 0.04$  eV,<sup>14</sup> and a prefactor,  $D_0 = 7.2 \times 10^{-4}$  cm<sup>2</sup>s<sup>-1</sup> was obtained. Above 250°C one observes a change in slope in the temperature dependence of the island density. For the temperature range corresponding to the images in Fig. 1, the ratio of hopping to deposition rate,  $h/r$ , varies over four orders of magnitude from  $1.2 \times 10^6$  to  $1.7 \times 10^{10}$ .

The self-similarity of the island size distributions seen in Fig. 1 is demonstrated more quantitatively by analyzing the size distributions obtained from the STM images. Figure 2 shows four island size distributions for temperatures ranging from 20 to 356°C. The island size distribution varies greatly with temperature due to the tendency towards enhanced growth with increasing temperature. This results in the peak of the distributions moving to

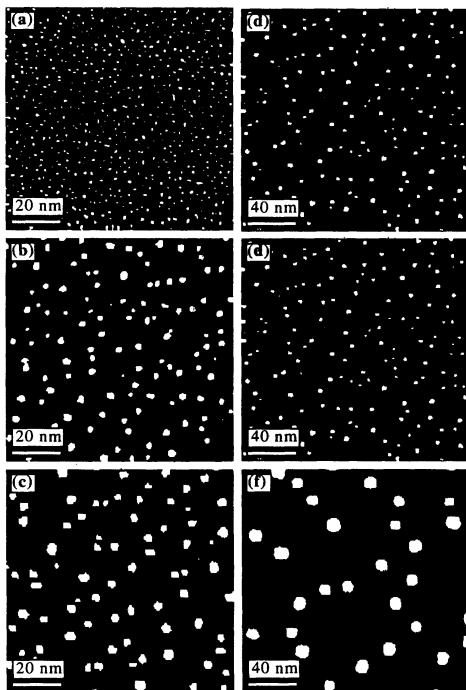


FIG. 1. STM images,  $100 \times 100$  nm<sup>2</sup>, of single-layer Fe islands (white) on the Fe(001) surface (black). Sample temperatures during growth are (a) 20°C, (b) 108°C, (c) 163°C, (d) 256°C, (e) 301°C, and (f) 356°C. Fe was deposited for a fixed time for all measurements with a flux of  $1.4 \pm 0.3 \times 10^{13}$  atoms cm<sup>-2</sup> s<sup>-1</sup>, yielding a coverage of  $0.07 \pm 0.016$  ML (1 ML =  $1.214 \times 10^{15}$  atoms cm<sup>-2</sup>).

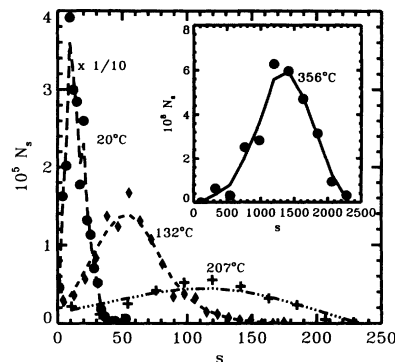


FIG. 2. Fe island size distributions corresponding to the STM images as in Fig. 1. The island density per lattice site ( $0.28 \times 0.28$  nm<sup>2</sup>)  $N_s$  is plotted vs the number of atoms (size)  $s$  per island for various growth temperatures indicated. The lines are a smooth spline to the data points.

larger island sizes with increasing temperature. Bartelt and Evans have developed a scaling theory for the island size distribution and propose the scaling relation for large  $h/r$  as<sup>9</sup>

$$N_s \sim \Theta_x s_{av}^{-2} f_i(s/s_{av}), \quad (2)$$

where  $N_s$  is the density of islands per lattice site of size  $s$  atoms, and  $f_i$  is the scaling function corresponding to a critical nucleus size  $i$ .  $\Theta_x = \sum_{s>i} s N_s$  is the coverage associated with stable islands and the average island size is defined as  $s_{av} = \Theta_x / \sum_{s>i} N_s$ . For a small critical size, such as  $i=1$ ,  $\Theta_x \approx \Theta$ , and  $s_{av} = \Theta_x / (N + N_1) \approx \Theta/N$ , since the relative number of monomers  $N_1$  is small compared to the total number of islands  $N$  ( $s \geq 2$ ).

Figure 3 shows the scaled island size distribution [which corresponds to the scaling function  $f$  in Eq. (2)] for the temperature range of 20–356°C, where the ratio of hopping rate to deposition rate ranges from  $10^6$  to  $10^{10}$ . For temperatures below 250°C [see Fig. 3(a)] one observes a *collapse* of the island size distributions onto a single curve, in excellent agreement with the relation given by Eq. (2). The resulting scaling function closely resembles the prediction for a critical size of 1, as can be seen by comparing to the simulation results of Bartelt and Evans,<sup>10</sup> which are reproduced in the inset in Fig. 3(a). This implies that clusters of two or more atoms are stable in this temperature range.

At higher growth temperatures, deviation from the scaling function in Fig. 3(a) is observed, as shown by the diamonds for the 301°C growth in Fig. 3(b). However, we observe that at yet higher growth temperatures (i.e., the data shown by the circles for 350°C growth) the island distributions still *collapse* onto the same curve, albeit a different scaling function curve than observed for the low-temperature growth. In contrast to the lower-temperature scaling function, this higher-temperature scaling function is significantly narrower and has a maximum greater than one. While coarsening due to Ostwald ripening would tend to narrow the size distribution, we expect little effect on the measured size distributions based on other coarsening measurements<sup>4</sup> and given the time and temperature scales in the present experiment. Therefore, we may attribute this distribution to a

second scaling function. At the temperature accompanying this new scaling function, we previously observed a marked decrease in total island density from the  $1/T$  behavior seen at lower temperatures, as shown in the inset in Fig. 3(b).<sup>5</sup>

The change to a different scaling function for the island size distributions at higher growth temperatures is suggestive of a change in critical size for nucleation.<sup>10</sup> Such a change would also lead to a slope change in the functional dependence of the total density on inverse temperature. A knowledge of the critical size would then allow a determination of the binding energy of the critical cluster, which is in general difficult to determine. Comparing to the simulation data of Bartelt and Evans,<sup>10</sup> the measured scaled size distribution qualitatively resembles the

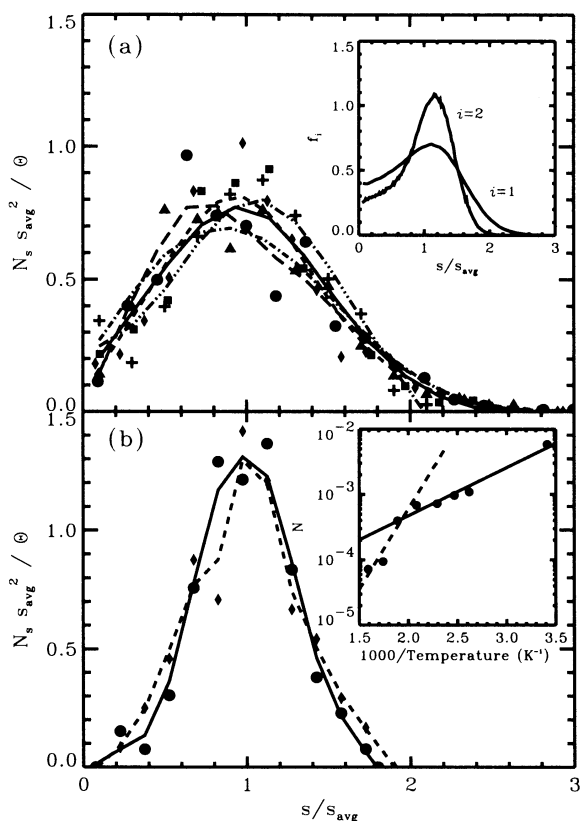


FIG. 3. Scaled island size distributions as a function of growth temperature from the STM measurements as in Fig. 1.  $N_s$  is the island density per lattice site of islands with  $s$  atoms and  $s_{av}$  is the average island size taken as  $\Theta/N$ , where  $\Theta$  is the total coverage and  $N$  the total island density. The lines are smooth splines to the data points, which are obtained from a histogram of the island distributions. (a) Lower-temperature data; the temperatures and ratio of hopping rate to deposition rate ( $h/r$ ) are (circles, solid line) 20°C,  $1.2 \times 10^6$ ; (squares, long dashed) 108°C,  $7.3 \times 10^7$ ; (diamonds, short dashed) 132°C,  $1.7 \times 10^8$ ; (triangles, dash-dot) 163°C,  $4.2 \times 10^8$ ; and (pluses, dash-triple dot) 207°C,  $1.3 \times 10^9$ . The inset shows the scaling functions determined by the simulations of Bartelt and Evans for  $h/r=10^6$  (Ref. 10). (b) Higher-temperature data; (diamonds, dashed) 301°C,  $7.7 \times 10^9$ ; (circles, solid) 356°C,  $1.7 \times 10^{10}$ . The inset shows the total island density per lattice site as a function of temperature. The solid and dashed lines are a fit to the data points below and above 250°C, respectively.

scaling functions for a critical size of 2, a seen in the inset of Fig. 3(a). For critical sizes greater than one, the dependence of the computed size distributions on the critical nucleus size is not strong enough to differentiate them; the measured high-temperature scaling function resembles the simulation results for a range in critical size between 2–4. However, further information is obtained from the total island density, shown in the inset in Fig. 3(b), which can be used to further discriminate the critical size.<sup>10</sup> From Eq. (1), computed values of the island density only compare favorably with the measured values for a critical size of  $i=3$ ; for example, at  $T=350^\circ\text{C}$ ,  $N(i=2)=5.2 \times 10^{-4}$ ,  $N(i=3)=2.5 \times 10^{-5}$ , and  $N(i=4)=3.2 \times 10^{-6}$ , whereas the experimental value is  $\sim 7 \times 10^{-5}$ . Thus we attribute the high-temperature scaling function to a critical island size of 3. The binding of the critical cluster can be estimated from the slope of the dashed line in the inset in Fig. 3(b), and yields a value of  $E_3=1.1 \pm 1.0$  eV,<sup>14</sup> corresponding to a bond energy of  $\sim 0.5$  eV. Further measurements and analysis, such as measuring the dependence of island density on deposition rate,<sup>15</sup> would be useful as a second determination of the critical size and the binding energy of the critical cluster.

The third feature noticed in the images of the Fe islands in Fig. 1 was the characteristic region around each island which is void of other islands. A more quantitative measure is obtained from the conditional probability distribution  $N(r)$  of finding an island (of any size) separated by  $r$  from a specified island. Figure 4 shows the radial separation distributions for the temperature range of 20–250°C. The lack of data at higher temperature is due to the lack of sufficient statistics (or islands) in the measured STM images at the higher temperatures. The scaling of the island separation distributions has been predicted by Bartelt and Evans in the limit of large  $h/r$  to be<sup>9</sup>

$$N(r) \sim N g_N [(r - r_0)/l_{av}], \quad (3)$$

where  $l_{av}$  is the characteristic separation between islands,  $l_{av} \sim \sqrt{1/N}$ , and  $r_0$  is the minimum separation where

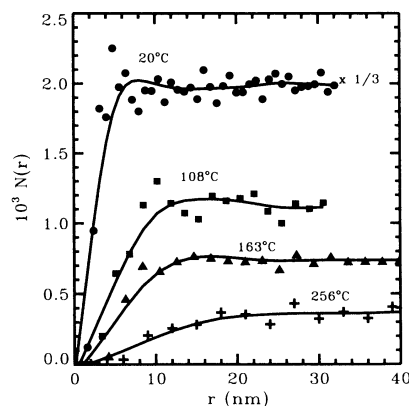


FIG. 4. Fe island separation distributions as a function of growth temperature from the STM images as in Fig. 1.  $N(r)$  is the conditional probability of finding an island (of any size) separated by  $r$  from a given island. The lines are a smooth spline to the data points.

$N(r)$  vanishes due to the finite island size.  $g_N$  has the property  $g_N \rightarrow 0, r \rightarrow r_0$  and  $g_N \rightarrow 1, r \rightarrow \infty$ . The scaled island separation distributions for the Fe on Fe data are shown in Fig. 5 for  $h/r$  ranging from  $10^6$  to  $10^9$ . One observes a collapse of the distributions onto a single curve in agreement with the predictions with the relation given by Eq. (3). A general characteristic of the scaling function for the separation distribution is a depletion of islands at small separations, which results from a lower nucleation probability in the vicinity of an existing island. This follows from the dependence of the nucleation probability on an atom finding a nearby adatom, together with the fact that the monomer density is zero at the edge of the island (the island acts as a sink for monomers) and increases as one goes away from the island. The functional form for the spatial dependence of the monomer density can be obtained from solving a two-dimensional diffusion equation;<sup>2,9</sup> this can be used to obtain an approximate expression for the scaling function for the separation distributions, as shown by the solid line in Fig. 5. One observes a reasonable agreement between the experimental data and the scaling function obtained from solving a continuum diffusion equation.

In summary, we have shown that the Fe island size and separation distributions obey scaling relations as a function of diffusion to deposition rate ranging from  $10^6$  to  $10^{10}$ , as recently predicted in nucleation and growth theories. A comparison of the scaling functions for the size distributions indicates a critical nucleus size of 1 is operative in the temperature range 20–250 °C. At higher temperature, a second scaling function was observed for the size distribution suggesting a change in critical cluster size.

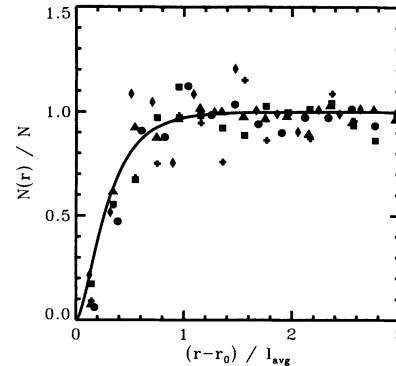


FIG. 5. Scaled radial separation distributions for finding an Fe island separated by a distance  $r$  from a given island obtained from the STM images as in Fig. 1. The growth temperatures and ratio of hopping rate to deposition rate are (circles) 20 °C,  $1.2 \times 10^6$ ; (squares) 108 °C,  $7.3 \times 10^7$ ; (diamonds) 132 °C,  $1.7 \times 10^8$ ; (triangles) 163 °C,  $4.2 \times 10^8$ ; and (pluses) 256 °C,  $3.5 \times 10^9$ .  $l_{av}$  is taken as  $1/\sqrt{N}$  and  $r_0/l_{av}$  as  $\sqrt{\Theta}$ . The solid line is given by  $\{1 - K_0[\lambda(y_0 + x)]/K_0(\lambda y_0)\}^2$  where  $K_0$  is the modified first-order Bessel function,  $x = (r - r_0)/l_{av}$ ,  $\lambda = \sqrt{4\pi}$ , and  $y_0 = r_0/l_{av} \sim \sqrt{\Theta} = 0.26$  (Ref. 9).

We are grateful to J. Evans, R. J. Celotta, and M. D. Stiles for helpful discussions, and R. A. Dragoset for his assistance. This work was supported by the Office of Technology Administration of the Department of Commerce and the Office of Naval Research. The Fe whiskers were grown at Simon Fraser University under an operating grant from the National Science and Engineering Research Council of Canada.

<sup>1</sup>See, for example, *Kinetics of Ordering and Growth at Surfaces*, Vol. 239 of *NATO Advanced Study Institute, Series B: Physics*, edited by M. Lagally (Plenum, New York, 1990).

<sup>2</sup>J. A. Venables, *Philos. Mag.* **27**, 697 (1973); J. A. Venables, G. D. Spiller, and M. Handbücken, *Rep. Prog. Phys.* **47**, 399 (1984).

<sup>3</sup>J. A. Venables, T. Doust, J. S. Drucker, and M. Krishnamurthy, in *Kinetics of Ordering and Growth at Surfaces* (Ref. 1), p. 437.

<sup>4</sup>Y.-W. Mo, J. Kleiner, M. B. Webb, and M. G. Lagally, *Phys. Rev. Lett.* **66**, 1998 (1991); *Surf. Sci.* **268**, 275 (1992).

<sup>5</sup>J. A. Stroschio, D. T. Pierce, and R. A. Dragoset, *Phys. Rev. Lett.* **70**, 3615 (1993); J. A. Stroschio and D. T. Pierce, *Proceedings of STM'93, Beijing, China, 1993* [*J. Vac. Sci. Technol. B* (to be published)].

<sup>6</sup>B. Voigtländer and A. Zinner, *Surf. Sci.* **292**, L775 (1993).

<sup>7</sup>E. Kopatzki, S. Günther, W. Nichtl-Pecher, and R. J. Behm, *Surf. Sci.* **284**, 154 (1993).

<sup>8</sup>J. A. Blackman and A. Wilding, *Europhys. Lett.* **16**, 115 (1991).

<sup>9</sup>M. C. Bartelt and J. W. Evans, *Phys. Rev. B* **46**, 12 675 (1992);

J. W. Evans and M. C. Bartelt, *Surf. Sci.* **284**, L437 (1993); M. C. Bartelt, M. C. Tringides, and J. W. Evans, *Phys. Rev. B* **47**, 13 891 (1993).

<sup>10</sup>M. C. Bartelt and J. W. Evans, *Surf. Sci.* **298**, 421 (1993); in *Commons Themes and Mechanisms of Epitaxial Growth*, MRS Symposia Proceedings No. 312 (Materials Research Society, Pittsburgh, 1993), p. 255; J. W. Evans and M. C. Bartelt, *J. Vac. Sci. Technol.* (to be published).

<sup>11</sup>C. Ratsch, A. Zangwill, P. Smilauer, and D. D. Vvedensky (unpublished).

<sup>12</sup>J. G. Amar, F. Family, and P.-M. Lam, in *Mechanisms of Thin Film Evolution*, MRS Symposia Proceedings No. 317 (Materials Research Society, Pittsburgh, 1994); *Phys. Rev. B* (to be published).

<sup>13</sup>J. A. Stroschio, D. T. Pierce, R. A. Dragoset, and P. N. First, *J. Vac. Sci. Technol. A* **10**, 1981 (1992).

<sup>14</sup>Uncertainty estimates are one standard deviation.

<sup>15</sup>H.-J. Ernst, F. Fabre, and J. Lapujoulade, *Phys. Rev. B* **46**, 1929 (1992).

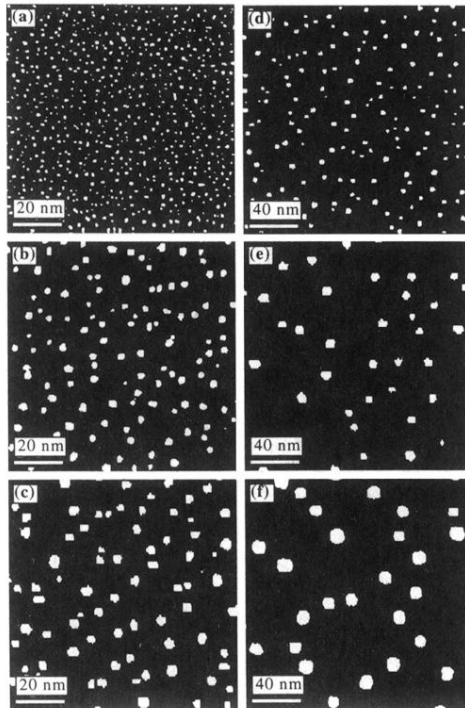


FIG. 1. STM images,  $100 \times 100 \text{ nm}^2$ , of single-layer Fe islands (white) on the Fe(001) surface (black). Sample temperatures during growth are (a)  $20^\circ\text{C}$ , (b)  $108^\circ\text{C}$ , (c)  $163^\circ\text{C}$ , (d)  $256^\circ\text{C}$ , (e)  $301^\circ\text{C}$ , and (f)  $356^\circ\text{C}$ . Fe was deposited for a fixed time for all measurements with a flux of  $1.4 \pm 0.3 \times 10^{13} \text{ atoms cm}^{-2} \text{ s}^{-1}$ , yielding a coverage of  $0.07 \pm 0.016 \text{ ML}$  ( $1 \text{ ML} = 1.214 \times 10^{15} \text{ atoms cm}^{-2}$ ).